



RARE CHARM DECAYS

Item Type	article
Authors	Golowich, Eugene
Download date	2025-05-01 02:35:16
Link to Item	https://hdl.handle.net/20.500.14394/41067

RARE CHARM DECAYS

EUGENE GOLOWICH

*Department of Physics, University of Massachusetts
Amherst MA 01003, USA*



This paper is a written version of a talk on rare (FCNC) D meson decays as presented at the Electroweak Moriond 2002. The presentation proceeds in two parts. We first consider Standard Model predictions, taking into account both short-distance and long distance effects. Then several New Physics options (*e.g.* supersymmetry, strong dynamics, extra large dimensions, *etc*) are considered.

1 Introductory Remarks

I dedicate this paper (as I did my talk) to Jean Tran Thanh Van and his wife for their valuable contributions over many years to our discipline.

My talk summarized a recent paper¹ written in collaboration with Gustavo Burdman, JoAnne Hewett and Sandip Pakvasa on the topic of rare flavor-changing neutral current (FCNC) decays of D mesons. Transitions of this class include: (i) $D \rightarrow V\gamma$ ($V = \rho, \omega, \phi, \dots$),^a (ii) $D \rightarrow X\ell^+\ell^-$ ($X = \pi, K, \eta, \rho, \omega, \phi, \dots$), (iii) $D \rightarrow X\nu_\ell\bar{\nu}_\ell$ ($X = \pi, K, \eta, \dots$), (iv) $D \rightarrow \gamma\gamma$, (v) $D \rightarrow \ell^+\ell^-$.

Perhaps the most noteworthy aspect of the above list is that, at the time of this writing, exactly *zero* FCNC events have been detected.³ We are optimistic that this situation will be rectified in the fairly near future. The database for charm-related physics continues to expand, and experiments at B-factories, hadron colliders and tau/charm facilities will soon achieve truly interesting sensitivities.

As such, one can reasonably imagine a future conference talk which announces the detection of a D meson FCNC transition. How to interpret such a signal? There is a commonly adopted procedure which should be followed. First one determines whether the Standard Model (SM) can explain the observed events. If not, one proceeds to consider a menu of New Physics models.

^aThe single-photon decays were considered previously by the authors in a separate paper.²

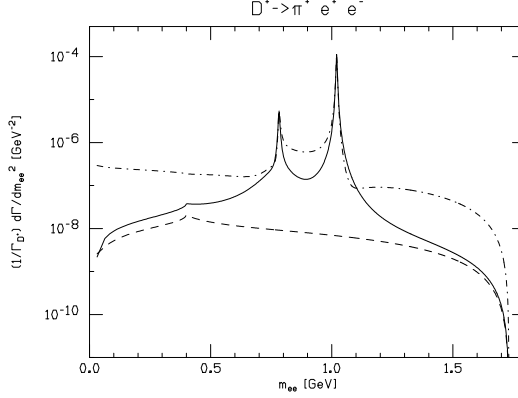


Figure 1: Dilepton mass distribution for $D^+ \rightarrow \pi^+ e^+ e^-$. The dashed (solid) line is the short-distance (total) SM contribution. The dot-dashed line is the R-parity violating contribution.

2 Standard Model Analysis

In principle, the task of producing SM predictions for FCNC D meson decays is straightforward. There are two components to the analysis, short-distance (SD) and long-distance (LD), which must be separately calculated. We consider each in turn.

2.1 The short-distance component

Short-distance amplitudes are concerned with the QCD degrees of freedom (quarks, gluons) and any relevant additional fields (leptons, photons). Thus, the short distance part of the $D \rightarrow X_u \ell^+ \ell^-$ amplitude involves the quark process $c \rightarrow u \ell^+ \ell^-$. It is usually most natural to employ an effective description in which the weak hamiltonian is expressed in terms of local multiquark operators and Wilson coefficients.⁴ For example, the effective hamiltonian for $c \rightarrow u \ell^+ \ell^-$ with renormalization scale μ in the range $m_b \geq \mu \geq m_c$ is^b

$$\mathcal{H}_{\text{eff}}^{c \rightarrow u \ell^+ \ell^-} = -\frac{4G_F}{\sqrt{2}} \left[\sum_{i=1}^2 \left(\sum_{q=d,s} C_i^{(q)}(\mu) \mathcal{O}_i^{(q)}(\mu) \right) + \sum_{i=3}^{10} C'_i(\mu) \mathcal{O}'_i(\mu) \right] . \quad (1)$$

In the above, $\mathcal{O}_{1,2}^{(q)}$ are four-quark current-current operators, \mathcal{O}'_{3-6} are the QCD penguin operators, \mathcal{O}_7 (\mathcal{O}_8) is the electromagnetic (chromomagnetic) dipole operator and $\mathcal{O}_{9,10}$ explicitly couple quark and lepton currents. For example, we have

$$\mathcal{O}'_7 = \frac{e}{16\pi^2} m_c (\bar{u}_L \sigma_{\mu\nu} c_R) F^{\mu\nu} , \quad \mathcal{O}'_9 = \frac{e^2}{16\pi^2} (\bar{u}_L \gamma_\mu c_L) (\bar{\ell} \gamma^\mu \ell) . \quad (2)$$

The famous Inami-Lim functions⁵ contribute to the Wilson coefficients C_{7-10} at scale $\mu = M_W$.

Figure 1 displays the predicted dilepton mass spectrum for $D^+ \rightarrow \pi^+ \ell^+ \ell^-$. Several distinct kinds of contributions are included. The short-distance SM component corresponds to the dashed line, which is seen to lie beneath the other two curves. For reference, we cite the *inclusive* ‘short distance’ branching ratio,

$$\mathcal{B}r_{D^+ \rightarrow X_u^+ e^+ e^-}^{(\text{sd})} \simeq 2 \times 10^{-8} . \quad (3)$$

^bQuantities with primes have had the explicit b -quark contributions integrated out

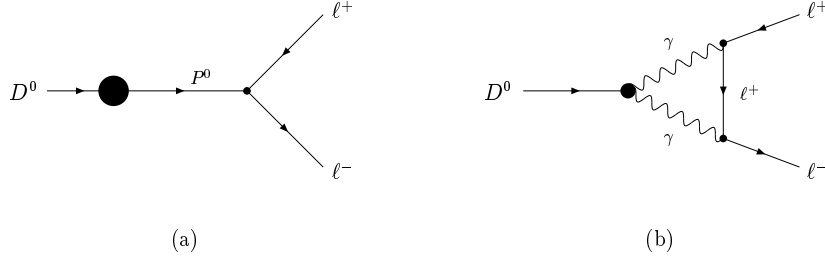


Figure 2: Long distance contributions to $D^0 \rightarrow \ell^+ \ell^-$.

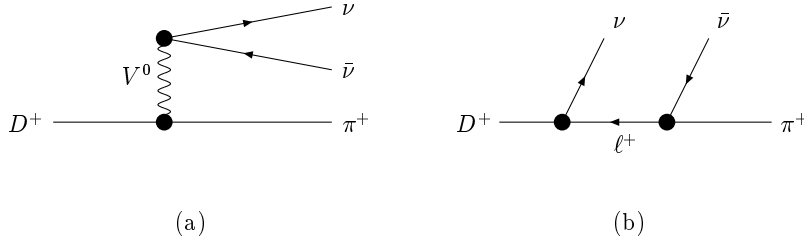


Figure 3: Long distance contributions to $D^+ \rightarrow \pi^+ \ell^+ \ell^-$.

2.2 The long-distance component

The long-distance component to a transition amplitude is often cast in terms of hadronic entities rather than the underlying quark and gluonic degrees of freedom. For charm decays, the long-distance amplitudes are typically important but difficult to determine with any rigor. There are generally several long-distance mechanisms for a given transition, *e.g.* as indicated for $D^0 \rightarrow \ell^+ \ell^-$ in Fig. 2 and for $D^+ \rightarrow \pi^+ \bar{\nu} \nu$ in Fig. 3.

Let us return to the case of $D^+ \rightarrow \pi^+ \ell^+ \ell^-$ depicted in Fig. 1. The solid curve represents the *total* SM signal, summed over both SD and LD contribution. In this case the LD component dominates, and from studying the dilepton mass distribution we can see what is happening. The peaks in the solid curve must correspond to intermediate resonances (ϕ , *etc*). The corresponding Feynman graph would be analogous to that in Fig. 3(a) in which the final state neutrino pair is replaced by a charged lepton pair. One finds numerically that

$$\mathcal{B}r_{D^+ \rightarrow \pi^+ e^+ e^-}^{(\text{SM})} \simeq \mathcal{B}r_{D^+ \rightarrow \pi^+ e^+ e^-}^{(\ell d)} \simeq 2 \times 10^{-6} \quad . \quad (4)$$

2.3 The Standard Model Predictions

Basing our analysis in part on existing literature,⁶ we have calculated both SD and LD amplitudes for a number of FCNC D transitions.¹ Results are collected in Table 1. As stated earlier, the current database for processes appearing in Table 1 consists entirely of upper bounds (or in the case of $D^0 \rightarrow \gamma \gamma$ no data entry at all). In all cases existing experimental bounds lie below the SM predictions, so there is no conflict between the two. For some (*e.g.* $D \rightarrow \pi \ell^+ \ell^-$) the gap between SM theory and experiment is not so large and there is hope for detection in the near future. In others (*e.g.* $D^0 \rightarrow \ell^+ \ell^-$) the gap is enormous, leaving ample opportunity for signals from New Physics to appear. This point is sometimes not fully appreciated and thus warrants some emphasis. It is why, for example, attempts to detect ΔM_D via D^0 - \bar{D}^0 mixing experiments are so important.

Table 1: Standard Model predictions and current experimental limits for the branching fractions due to short and long distance contributions for various rare D meson decays.

Decay Mode	Experimental Limit	$\mathcal{B}r_{S.D.}$	$\mathcal{B}r_{L.D.}$
$D^+ \rightarrow X_u^+ e^+ e^-$		2×10^{-8}	
$D^+ \rightarrow \pi^+ e^+ e^-$	$< 4.5 \times 10^{-5}$		2×10^{-6}
$D^+ \rightarrow \pi^+ \mu^+ \mu^-$	$< 1.5 \times 10^{-5}$		1.9×10^{-6}
$D^+ \rightarrow \rho^+ e^+ e^-$	$< 1.0 \times 10^{-4}$		4.5×10^{-6}
$D^0 \rightarrow X_u^0 + e^+ e^-$		0.8×10^{-8}	
$D^0 \rightarrow \pi^0 e^+ e^-$	$< 6.6 \times 10^{-5}$		0.8×10^{-6}
$D^0 \rightarrow \rho^0 e^+ e^-$	$< 5.8 \times 10^{-4}$		1.8×10^{-6}
$D^0 \rightarrow \rho^0 \mu^+ \mu^-$	$< 2.3 \times 10^{-4}$		1.8×10^{-6}
$D^+ \rightarrow X_u^+ \nu \bar{\nu}$		1.2×10^{-15}	
$D^+ \rightarrow \pi^+ \nu \bar{\nu}$			5×10^{-16}
$D^0 \rightarrow \bar{K}^0 \nu \bar{\nu}$			2.4×10^{-16}
$D_s \rightarrow \pi^+ \nu \bar{\nu}$			8×10^{-15}
$D^0 \rightarrow \gamma\gamma$		4×10^{-10}	$\text{few} \times 10^{-8}$
$D^0 \rightarrow \mu^+ \mu^-$	$< 3.3 \times 10^{-6}$	1.3×10^{-19}	$\text{few} \times 10^{-13}$
$D^0 \rightarrow e^+ e^-$	$< 1.3 \times 10^{-5}$	$(2.3 - 4.7) \times 10^{-24}$	
$D^0 \rightarrow \mu^\pm e^\mp$	$< 8.1 \times 10^{-6}$	0	0
$D^+ \rightarrow \pi^+ \mu^\pm e^\mp$	$< 3.4 \times 10^{-5}$	0	0
$D^0 \rightarrow \rho^0 \mu^\pm e^\mp$	$< 4.9 \times 10^{-5}$	0	0

3 New Physics Analysis

At this time, there is a wide collection of possible New Physics models leading to FCNC D transitions. Among those considered in Ref. 1 are (i) Supersymmetry (SUSY): R-parity conserving, R-parity violating, (ii) Extra Degrees of Freedom: Higgs bosons, Gauge bosons, Fermions, Spatial dimensions, (iii) Strong Dynamics: Extended technicolor, Top-condensation.

Due to limitations of time (for the talk) and space (for this summary) we restrict most of our attention to the case of supersymmetry. However, at the end we also make a few remarks on the topic of large extra dimensions. The SUSY discussion divides naturally according to how the R-parity R_P is treated, where

$$R_P = (-)^{3(B-L)+2S} = \begin{cases} +1 & (\text{particle}) \\ -1 & (\text{sparticle}) \end{cases} . \quad (5)$$

3.1 R-parity conserving SUSY

R-parity conserving SUSY will contribute to charm FCNC amplitudes via loops. For a penguin-like amplitude whose external lines are SM particles, the internal lines can be (i) gluino-squark pairs, (ii) charged Higgs-quark pairs or (iii) chargino/neutralino-squark pairs. Case (i) is the one considered here as case (ii) will be suppressed for the same CKM reason as in the SM and case (iii) is relatively suppressed to (i) because the vertices are weak-interaction rather than strong-interaction.

To calculate R-parity conserving SUSY contributions, we employ the so-called *mass insertion approximation*,⁷ which is oriented towards phenomenological studies and is also model independent. Let us first describe what is actually done and then provide a brief explanation of the underlying rationale.

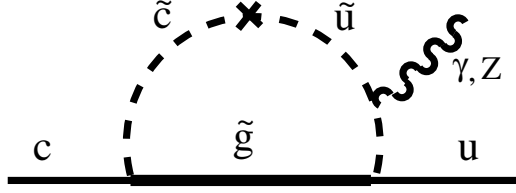


Figure 4: A typical contribution to $c \rightarrow u$ FCNC transitions in the MSSM. The cross denotes one mass insertion $(\delta_{12}^u)_{\lambda\lambda'}$ and λ, λ' are helicity labels.

In this approach, a squark propagator becomes modified by a mass insertion (*e.g.* the ‘ \times ’ in Fig. 4) that changes the squark flavor.^{7,8} For convenience, one expands the squark propagator in powers of the dimensionless quantity $(\delta_{ij}^u)_{\lambda\lambda'}$,

$$(\delta_{ij}^u)_{\lambda\lambda'} = \frac{(M_{ij}^u)_{\lambda\lambda'}^2}{M_{\tilde{q}}^2}, \quad (6)$$

where $i \neq j$ are generation indices, λ, λ' denote the chirality, $(M_{ij}^u)^2$ are the off-diagonal elements of the up-type squark mass matrix and $M_{\tilde{q}}$ represents the average squark mass. The exchange of squarks in loops thus leads to FCNC through diagrams such as the one in Fig. 4. The role of experiment is to either detect the predicted (SUSY-induced) FCNC signal or to constrain the contributing $(\delta_{ij}^u)_{\lambda\lambda'}$.

This topic is actually part of the super-CKM problem. If one works in a basis which diagonalizes the fermion mass matrices, then sfermion mass matrices (and thus sfermion propagators) will generally be nondiagonal. As a result, flavor changing processes can occur. One can use phenomenology to restrict these FCNC phenomena. The $Q = -1/3$ sector has yielded fairly strong constraints but thus far only D^0 - \bar{D}^0 mixing has been used to limit the $Q = +2/3$ sector. In our analysis, we have taken charm FCNCs to be as large as allowed by the D -mixing upper bounds.

For the decays $D \rightarrow X_u \ell^+ \ell^-$ discussed earlier in Sect. 2.1, the gluino contributions will occur additively relative to those from the SM and so we can write for the Wilson coefficients,

$$C_i = C_i^{(\text{SM})} + C_i^{\tilde{g}}. \quad (7)$$

To get some feeling for dependence on the $(\delta_{12}^u)_{\lambda\lambda'}$ parameters, we display the examples

$$C_7^{\tilde{g}} \propto (\delta_{12}^u)_{\text{LL}} \text{ and } (\delta_{12}^u)_{\text{LR}}, \quad C_9^{\tilde{g}} \propto (\delta_{12}^u)_{\text{LL}}, \quad (8)$$

whereas for quark helicities opposite^c to those in the operators of Eq. (2), one finds

$$\hat{C}_7^{\tilde{g}} \propto (\delta_{12}^u)_{\text{RR}} \text{ and } (\delta_{12}^u)_{\text{LR}}, \quad \hat{C}_9^{\tilde{g}} \propto (\delta_{12}^u)_{\text{RR}}. \quad (9)$$

Moreover, the term in $\hat{C}_7^{\tilde{g}}$ which contains $(\delta_{12}^u)_{\text{LR}}$ experiences the enhancement factor $M_{\tilde{g}}/m_c$.

We have numerically studied the effects in $c \rightarrow u \ell^+ \ell^-$ for the range of masses: (I) $M_{\tilde{g}} = M_{\tilde{q}} = 250$ GeV, (II) $M_{\tilde{g}} = 2 M_{\tilde{q}} = 500$ GeV, (III) $M_{\tilde{g}} = M_{\tilde{q}} = 1000$ GeV and (IV) $M_{\tilde{g}} = (1/2) M_{\tilde{q}} = 250$ GeV. For some modes in $D \rightarrow X_u \ell^+ \ell^-$, the effect of the squark-gluino contributions can be large relative to the SM component, both in the total branching ratio and for certain kinematic regions of the dilepton mass. The mode $D^0 \rightarrow \rho^0 e^+ e^-$ is given in Fig. 5. This figure should make clear the importance of measuring the low $m_{\ell^+ \ell^-}$ part of the dilepton mass spectrum.

^cWe use the notation \hat{C} for the associated Wilson coefficients.

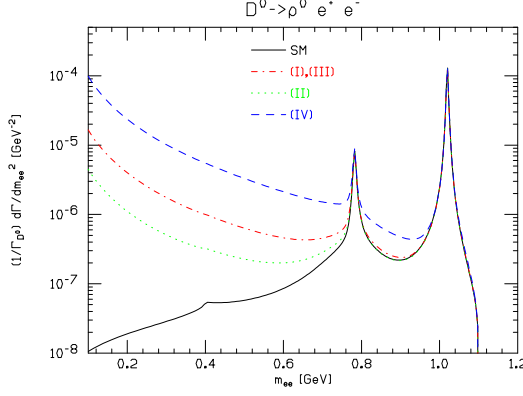


Figure 5: Dilepton mass distributions for $D^0 \rightarrow \rho^0 e^+ e^-$ in the mass insertion approximation of MSSM. The SM prediction (solid curve) is provided for reference and the MSSM curves refer to (i) $M_{\tilde{g}} = M_{\tilde{q}} = 250$ GeV, (ii) $M_{\tilde{g}} = 2M_{\tilde{q}} = 500$ GeV, (iii) $M_{\tilde{g}} = M_{\tilde{q}} = 1000$ GeV and (iv) $M_{\tilde{g}} = M_{\tilde{q}}/2 = 250$ GeV.

3.2 R -parity violating SUSY

The effect of assuming that R -parity can be violated is to allow additional interactions between particles and sparticles. Ignoring bilinear terms which are not relevant to our discussion of FCNC effects, we introduce the R -parity violating (RPV) super-potential of trilinear couplings,

$$\mathcal{W}_{\mathcal{R}_p} = \epsilon_{ab} \left[\frac{1}{2} \lambda_{ijk} L_i^a L_j^b \bar{E}_k + \lambda'_{ijk} L_i^a Q_j^b \bar{D}_k + \frac{1}{2} \epsilon_{\alpha\beta\gamma} \lambda''_{ijk} \bar{U}_i^\alpha \bar{D}_j^\beta \bar{D}_k^\gamma \right], \quad (10)$$

where L , Q , \bar{E} , \bar{U} and \bar{D} are the standard chiral super-fields of the MSSM and i, j, k are generation indices. The quantities λ_{ijk} , λ'_{ijk} and λ''_{ijk} are *a priori* arbitrary couplings which total $9 + 27 + 9 = 45$ unknown parameters in the theory.

For our purposes, the presence of RPV means that *tree-level* amplitudes become possible in which a virtual sparticle propagates from one of the trilinear vertices in Eq. (10) to another. In order to avoid significant FCNC signals (which would be in contradiction with current experimental limits), bounds must be placed on the (unknown) coupling parameters. As experimental probes become more sensitive, the bounds become ever tighter. In particular, the FCNC sector probed by charm decays involves the $\{\lambda'_{ijk}\}$. Introducing matrices \mathcal{U}_L , \mathcal{D}_R to rotate left-handed up-quark fields and right-handed down-quark fields to the mass basis, we obtain for the relevant part of the superpotential

$$\mathcal{W}_{\lambda'} = \tilde{\lambda}'_{ijk} \left[-\tilde{e}_L^i \bar{d}_R^k u_L^j - \tilde{u}_L^j \bar{d}_R^k e_L^i - (\bar{d}_R^k)^* (e_L^i)^c u_L^j + \dots \right], \quad (11)$$

where neutrino interactions are not shown and we define

$$\tilde{\lambda}'_{ijk} \equiv \lambda'_{irs} \mathcal{U}_{rj}^L \mathcal{D}_{sk}^{*R}. \quad (12)$$

Some bounds on the $\{\tilde{\lambda}'_{ijk}\}$ are already available from data on such diverse sources as charged-current universality, the ratio $\Gamma_{\pi \rightarrow e \nu_e} / \Gamma_{\pi \rightarrow \mu \nu_\mu}$, the semileptonic decay $D \rightarrow K \ell \nu_\ell$, *etc.*¹⁰ We have considered additional experimental implications of the preceding formalism:

(i) For the decay $D^+ \rightarrow \pi^+ e^+ e^-$, we display the effect of RPV as the dot-dash line in Fig. 1. Here, the effect is proportional to $\tilde{\lambda}'_{11k} \cdot \tilde{\lambda}'_{12k}$ and we have employed existing limits on these couplings. Although the effect on the branching ratio is not large, but the dilepton spectrum away from resonance poles is seen to be sensitive to the RPV contributions. This case is not optimal because the current experimental limit on $\mathcal{B}r_{D^+ \rightarrow \pi^+ e^+ e^-}$ is well above the dot-dash curve.

(ii) For $D^+ \rightarrow \pi^+ \mu^+ \mu^-$, the current experimental limit on $\mathcal{B}r_{D^+ \rightarrow \pi^+ \mu^+ \mu^-}$ actually provides the new bound

$$\tilde{\lambda}'_{11k} \cdot \tilde{\lambda}'_{12k} \leq 0.004 \quad . \quad (13)$$

(iii) Another interesting mode is $D^0 \rightarrow \mu^+ \mu^-$. Upon using the bound of Eq. (13) we obtain

$$\mathcal{B}r_{D^0 \rightarrow \mu^+ \mu^-}^{\mathcal{R}p} < 3.5 \times 10^{-6} \left(\frac{\tilde{\lambda}'_{12k}}{0.04} \right)^2 \left(\frac{\tilde{\lambda}'_{11k}}{0.02} \right)^2 \quad . \quad (14)$$

A modest improvement in the existing limit on $\mathcal{B}r_{D^0 \rightarrow \mu^+ \mu^-}$ will yield a new bound on the product $\tilde{\lambda}'_{11k} \cdot \tilde{\lambda}'_{12k}$.

(iv) Lepton flavor violating processes are allowed by the RPV lagrangian. One example is the mode $D^0 \rightarrow e^+ \mu^-$, for which existing parameter bounds predict

$$\mathcal{B}r_{D^0 \rightarrow \mu^+ e^-}^{\mathcal{R}p} < 0.5 \times 10^{-6} \times \left[\left(\frac{\tilde{\lambda}'_{11k}}{0.02} \right) \left(\frac{\tilde{\lambda}'_{22k}}{0.21} \right) + \left(\frac{\tilde{\lambda}'_{21k}}{0.06} \right) \left(\frac{\tilde{\lambda}'_{12k}}{0.04} \right) \right] \quad . \quad (15)$$

An order-of-magnitude improvement in $\mathcal{B}r_{D^0 \rightarrow \mu^+ e^-}^{\mathcal{R}p}$ will provide a new bound on the above combination of RPV couplings.

3.3 Large Extra Dimensions

For several years, the study of large extra dimensions ('large' means much greater than the Planck scale) has been an area of intense study. This approach might hold the solution of the hierarchy problem while having verifiable consequences at the TeV scale or less. Regarding the subject of rare charm decays, one's reaction might be to ask *How could extra dimensions possibly affect the decays of ordinary hadrons?* We provide a few examples in the following.

Suppose the spacetime of our world amounts to a 3+1 brane which together with a manifold of additional dimensions (the bulk) is part of some higher-dimensional space. A field Θ which can propagate in a large extra dimension will exhibit a Kaluza-Klein (KK) tower of states $\{\Theta_n\}$, detection of which would signal existence of the extra dimension. Given our ignorance regarding properties of the bulk or of which fields are allowed to propagate in it, one naturally considers a variety of different models.

Assume, for example, the existence of an extra dimension of scale $1/R \sim 10^{-4}$ eV such that the gravitational field (denote it simply as G) alone can propagate in the extra dimension.¹¹ There are then bulk-graviton KK states $\{G_n\}$ which couple to matter. In principle there will be the FCNC transitions $c \rightarrow u G_n$ and since the $\{G_n\}$ remain undetected, there will be apparent missing energy. However this mechanism leads to too small a rate to be observable.

Another possibility which has been studied is that the scale of the extra dimension is $1/R \sim 1$ TeV and that SM gauge fields propagate in the bulk.¹² However, precision electroweak data constrain the mass of the first gauge KK excitation to be in excess of 4 TeV¹³, and hence their contributions to rare decays are small¹⁴.

More elaborate constructions, such as allowing fermion fields to propagate in the five-dimensional bulk of the Randall-Sundrum localized-gravity model¹⁵, are currently being actively explored.¹⁶ Interesting issues remain and a good deal more study deserves to be done.

4 Concluding Remarks

In the Standard Model, FCNC processes are suppressed. Both photon and Z-boson SM vertices are flavor diagonal, so tree level diagrams involving virtual propagation of these particles will not contribute to FCNC processes. One must instead consider loops. As regards FCNC processes,

SM loops are largest for kaon and B-meson transitions due mainly to the large t -quark mass and also to favorable CKM dependence. The upshot is that studies of FCNC processes for charm have lagged behind those of the other flavors. There is of course a basic irony in this – it is precisely because SM signals are expected to be so small for charm FCNC that the opportunity for evidence of New Physics to emerge becomes enhanced relative to the other flavors. The situation begs for experimental input.

Acknowledgments

The work described in this talk was supported in part by the National Science Foundation under Grant PHY-9801875.

References

1. G. Burdman, E. Golowich, J. Hewett and S. Pakvasa, Phys. Rev. D (to be published); hep-ph/0112235 v2.
2. G. Burdman, E. Golowich, J. Hewett and S. Pakvasa, Phys. Rev. **D52**, 6383 (1995).
3. D.E. Groom *et al.*, Particle Data Group, Eur. Phys. J. **C15**, 1 (2000) and updated PDG database accessed via the Web at *pdg.lbl.gov*.
4. G. Buchalla, A. J. Buras and M. E. Lautenbacher, Rev. Mod. Phys. **68**, 1125 (1996).
5. T. Inami and C.S. Lim, Prog. Theor. Phys. **65**, 1772 (1981).
6. Such references include C. Greub *et al.*, Phys. Lett. **B382**, 415 (1996); C-H. V. Chang, G-L. Lin and Y-P. Yao, Phys. Lett. **B415**, 395 (1997); L. Reina, G. Ricciardi and A. Soni, Phys. Rev. **D56**, 5805 (1997); D. Choudhury and J. Ellis, Phys. Lett. **B433**, 102 (1998); S. Fajfer, P. Singer and J. Zupan, Phys. Rev. **D64**, 074008 (2001); C. S. Lim, T. Morozumi and A. I. Sanda, Phys. Lett. **B218**, 343 (1989); N.G. Deshpande, J. Trampetic, and K. Panrose, Phys. Rev. **D39**, 1461 (1989); P. Singer and D.-X. Zhang, Phys. Rev. **D55**, R1127 (1997).
7. L.J. Hall, V.A. Kostelecky, and S. Raby, Nucl. Phys. **B267**, 415 (1986).
8. For a comprehensive study of FCNC effects in supersymmetry see, S. Bertolini, F. Borzumati, A. Masiero, and G. Ridolfi, Nucl. Phys. **B193**, 591 (1991); F. Gabbiani, E. Gabrielli, A. Masiero and L. Silvestrini, Nucl. Phys. **B477**, 321 (1996); J.L. Hewett and J.D. Wells, Phys. Rev. **D55**, 5549 (1997); P. Cho, M. Misiak, and D. Wyler, Phys. Rev. **D54**, 3329 (1996). For a review see M. Misiak, S. Pokorski and J. Rosiek, in “*Heavy Flavors II*”, eds. A.J. Buras and M. Lindner, Adv. Ser. Direct. High Energy Phys. **15**, 795 (1998).
9. *E.g.*, see J. Ellis and D.V. Nanopoulos, Phys. Lett. **110B**, 44 (1982).
10. For a recent review, see, B. C. Allanach, A. Dedes and H. K. Dreiner, Phys. Rev. **D60**, 075014 (1999).
11. N. Arkani-Hamed, S. Dimopoulos, and G. Dvali, Phys. Lett. **B429**, 263 (1998), and Phys. Rev. **D59**, 086004 (1999); I. Antoniadis, N. Arkani-Hamed, S. Dimopoulos, and G. Dvali, Phys. Lett. **B436**, 257 (1998).
12. I. Antoniadis, Phys. Lett. **B246**, 377 (1990); J. Lykken, Phys. Rev. **D54**, 3693 (1996); E. Witten, Nucl. Phys. **B471**, 135 (1996); P. Horava and E. Witten, Nucl. Phys. **B460**, 506 (1996), *ibid.*, **B475**, 94 (1996).
13. T.G. Rizzo and J.D. Wells, Phys. Rev. **D61**, 016007 (2000); P. Nath and M. Yamaguchi, Phys. Rev. **D60**, 116006 (1999); M. Masip and A. Pomarol, Phys. Rev. **D60**, 096005 (1999); W.J. Marciano, Phys. Rev. **D60**, 093006 (1999).
14. See, for example, K. Agashe, N.G. Deshpande, G.H. Wu, Phys. Lett. **B514**, 309 (2001).
15. L. Randall and R. Sundrum, Phys. Rev. Lett. **83**, 3370 (1999), and *ibid.*, 4690, (1999).
16. J.L. Hewett, F.J. Petriello, and T.G. Rizzo, SLAC-PUB-9146; arXiv:hep-ph/0203091.